Available online at www.sciencedirect.com
ScienceDirect
International Journal of Engineering Science 45 (2007) 173–184
International Journal of Engineering Science
www.elsevier.com/locate/ijengsci

Non-orthogonal stagnation-point flow of a micropolar fluid

Y.Y. Lok [a], I. Pop [b,*], Ali J. Chamkha [c]

[a] *Centre for Academic Services, Kolej Universiti Teknikal Kebangsaan Malaysia, 75450 Ayer Keroh, Melaka, Malaysia*
[b] *Faculty of Mathematics, University of Cluj, R-3400 Cluj, CP 253, Romania*
[c] *Manufacturing Engineering Department, The Public Authority for Applied Education and Training, Shuweikh 70654, Kuwait*

Received 26 October 2005; received in revised form 22 March 2006; accepted 13 April 2006
Available online 13 November 2006

Abstract

This paper considers the problem of steady two-dimensional flow of a micropolar fluid impinging obliquely on a flat plate. The flow under consideration is a generalization of the classical modified Hiemenz flow for a micropolar fluid which occurs in the boundary layer near an orthogonal stagnation point. A coordinate decomposition transforms the full governing equations into a primary equation describing the modified Hiemenz flow for a micropolar fluid and an equation for the tangential flow coupled to the primary solution. The solution to the boundary-value problem is governed by two non-dimensional parameters: the material parameter K and the ratio of the microrotation to skin friction parameter n. The obtained ordinary differential equations are solved numerically for some values of the governing parameters. The primary consequence of the free stream obliqueness is the shift of the stagnation point toward the incoming flow.

1. Introduction

Great interest in micropolar fluids, which exhibit the microrotational effects and microrotational inertia, began very soon after the pioneering studies by Eringen [1,2]. Hoyt and Fabula [3] have shown experimentally that fluids which cannot be characterized by Newtonian relationships, namely fluids containing minute polymeric additives indicate considerable reduction of the skin friction near a rigid body (about 25–30%), and it can be well explained by the theory of micropolar fluids. Eringen's micropolar model includes the classical Navier–Stokes equations as a special case, but can cover, both in theory and applications, many more, phenomena than the classical model. Among the interesting results that Eringen has cited were the occurrence of a thermodynamic pressure tensor, the coupling of the temperature gradient with the constitutive equations and the occurrence of the microrotation vector in the heat conduction equation. None of these effects were present in the classical field theories of fluids. In practice, the theory of micropolar fluids require that one must solve an additional transport equation representing the principle of conservation of local angular momentum, as well as

* Corresponding author. Tel.: +40 264 594315; fax: +40 264 591906.
E-mail address: pop.ioan@yahoo.co.uk (I. Pop).

0020-7225/$ - see front matter © 2006 Elsevier Ltd. All rights reserved.
doi:10.1016/j.ijengsci.2006.04.016

Nomenclature

a	constant in Eq. (6)
A	constant in Eq. (27)
C_f	skin friction coefficient
j	microinertia density
K	material parameter
n	ratio of the microrotation vector component and the fluid skin friction at the wall
$\bar{N}$	component of the microrotation vector normal to $\bar{x}$–$\bar{y}$ plane
N	non-dimensional component of the microrotation vector normal to x–y plane
$\bar{p}$	pressure
P	non-dimensional pressure
$\bar{u}, \bar{v}$	velocity components along $\bar{x}$- and $\bar{y}$-axes
u, v	non-dimensional velocity components along x- and y-axes
$\bar{x}, \bar{y}$	Cartesian coordinates along the plate and normal to it, respectively
x, y	non-dimensional Cartesian coordinates along the wall and normal to it, respectively

Greek symbols

α	constant in Eq. (28)
γ	spin gradient viscosity
η	similarity variable
κ	vortex viscosity
λ	characteristic length of the flat plate
μ	dynamic viscosity
ν	kinematic viscosity
ρ	density
$\bar{\tau}_w$	skin friction at the plate
τ_w	non-dimensional skin friction at the plate
ψ	non-dimensional stream function at the plate

Subscripts

w	wall condition
∞	far field condition

the usual transport equations for the conservation of mass and momentum, and additional constitutive parameters are also introduced. Examples of industrially relevant flows that can be studied using the micropolar theory include the flow of low concentration suspensions, liquid crystals, animal blood, colloidal fluids, lubrication, turbulent shear flow, etc. Since the publication of Eringen's micropolar fluid theory, many authors have investigated various flow and heat transfer problems. Extensive reviews of the theory and applications can be found in the review articles by Ariman et al. [4,5] and the recent books by Łukaszewicz [6] and Eringen [7].

Here we analyse the steady two dimensional stagnation-point flow of a micropolar fluid impinging on a flat rigid wall obliquely. This flow appears when a jet of viscous fluids impinges on a rigid wall obliquely. In many cases, the jet may be oblique to the impinged surface due to surface contouring or physical constraints on the nozzle [8]. In particular, we investigate the behaviour of the micropolar fluid near the wall for various values of the micropolar parameter and rate of particle rotation to the skin friction at the plate. The objective of our paper is also to show that an exact solution of the governing equations can be obtained, which represents the classical steady Hiemenz [9] flow past a flat plate immersed in a micropolar fluid. From a mathematical point of view, this problem is of interest because it represents, for the case of a Newtonian fluid, one of the relatively few instances in fluid mechanics where an exact closed form solution can be obtained. The existence of the exact Newtonian flow solution greatly facilitates an analysis of results from the study of the correspond-

ing micropolar flow problem, in so much as one is able to highlight more easily the differences between the micropolar and classical Hiemenz flow.

It is worth mentioning that the two-dimensional stagnation-point flow is an interesting problem in the history of fluid mechanics. Hiemenz [9] derived an exact solution of the Navier–Stokes equations which describes the steady flow directed perpendicularly to an infinite flat plate. Stuart [10], Tamada [11], Dorrepaal [12] and Labropulu et al. [13] have extended the classical steady Hiemenz to oblique stagnation-point flow, while Wang [8] and Takemitsu and Matunobu [14] presented exact solutions of the unsteady oblique stagnation-point flow. Dorrepaal et al. [15] investigated the behaviour of a steady visco-elastic fluid impinging on a flat rigid wall at an arbitrary angle of incidence and found that the ratio of the two slopes depends upon the elastic effects of the fluid but it is independent of the angle of incidence of the streamline. Finally, we mention that Tilley and Weidman [16] have studied the steady oblique two-fluid stagnation-point flow.

2. Basic equations

Consider the steady two-dimensional flow of a micropolar fluid near a non-orthogonal stagnation point at a fixed flat plate coinciding with the plane $\bar{y}=0$, the flow being confined to $\bar{y}>0$. Cartesian coordinates $(\bar{x},\bar{y})$ fixed in space are taken, the $\bar{x}$-axis being along the plate and the $\bar{y}$-axis normal to it, respectively. The steady two-dimensional flow of a micropolar fluid is described by the following equations:

$$\frac{\partial \bar{u}}{\partial \bar{x}}+\frac{\partial \bar{v}}{\partial \bar{y}}=0 \tag{1}$$

$$\bar{u}\frac{\partial \bar{u}}{\partial \bar{x}}+\bar{v}\frac{\partial \bar{u}}{\partial \bar{y}}=-\frac{1}{\rho}\frac{\partial \bar{p}}{\partial \bar{x}}+\left(\frac{\mu+\kappa}{\rho}\right)\bar{\nabla}^2\bar{u}+\frac{\kappa}{\rho}\frac{\partial \bar{N}}{\partial \bar{y}} \tag{2}$$

$$\bar{u}\frac{\partial \bar{v}}{\partial \bar{x}}+\bar{v}\frac{\partial \bar{v}}{\partial \bar{y}}=-\frac{1}{\rho}\frac{\partial \bar{p}}{\partial \bar{y}}+\left(\frac{\mu+\kappa}{\rho}\right)\bar{\nabla}^2\bar{v}-\frac{\kappa}{\rho}\frac{\partial \bar{N}}{\partial \bar{x}} \tag{3}$$

$$\rho j\left(\bar{u}\frac{\partial \bar{N}}{\partial \bar{x}}+\bar{v}\frac{\partial \bar{N}}{\partial \bar{y}}\right)=\gamma\bar{\nabla}^2\bar{N}-\kappa\left(2\bar{N}+\frac{\partial \bar{u}}{\partial \bar{y}}-\frac{\partial \bar{v}}{\partial \bar{x}}\right) \tag{4}$$

where $\bar{u}$ and $\bar{v}$ are the velocity components along the $\bar{x}$- and $\bar{y}$-axes, respectively, $\bar{N}$ is the component of the microrotation vector normal to the $\bar{x}$–$\bar{y}$ plane, ρ is the density, μ is the absolute viscosity, κ is the vortex viscosity, γ is the spin-gradient viscosity, j is the microinertia density and $\bar{\nabla}^2$ is the Laplacian in Cartesian coordinates $(\bar{x},\bar{y})$. It is assumed that all physical quantities ρ, μ, κ, γ and j are constants. We follow the work of many recent authors by assuming that γ is given by, see Rees and Bassom [17] or Rees and Pop [18]

$$\gamma=(\mu+\kappa/2)j=\mu(1+K/2)j \tag{5}$$

with $K=\kappa/\mu$ being the material parameter. We introduce now the following non-dimensional variables:

$$\begin{aligned} &x=\bar{x}/\lambda,\quad y=\bar{y}/\lambda,\quad u=(\lambda/\nu)\bar{u},\quad v=(\lambda/\nu)\bar{v}\\ &N=\bar{N}/a,\quad p=\bar{p}/(\rho a^2\lambda^2)\end{aligned} \tag{6}$$

where λ is a characteristic length of the flat plate and $a=\nu/\lambda^2$ (>0) is a constant which has units of inverse time. Substituting (6) into Eqs. (1)–(4), they become

$$\frac{\partial u}{\partial x}+\frac{\partial v}{\partial y}=0 \tag{7}$$

$$u\frac{\partial u}{\partial x}+v\frac{\partial u}{\partial y}=-\frac{\partial p}{\partial x}+(1+K)\nabla^2u+K\frac{\partial N}{\partial y} \tag{8}$$

$$u\frac{\partial v}{\partial x}+v\frac{\partial v}{\partial y}=-\frac{\partial p}{\partial y}+(1+K)\nabla^2v-K\frac{\partial N}{\partial x} \tag{9}$$

$$u\frac{\partial N}{\partial x}+v\frac{\partial N}{\partial y}=(1+K/2)\nabla^2N-K\left(2N+\frac{\partial u}{\partial y}-\frac{\partial v}{\partial x}\right) \tag{10}$$

where $j=\lambda^2$ defines the length scale, λ, see Rees and Bassom [17].

Further, we introduce the stream function ψ defined as

$$u = \frac{\partial \psi}{\partial y}, \quad v = -\frac{\partial \psi}{\partial x} \tag{11}$$

and eliminate pressure p from Eqs. (8) and (9). Thus, we get

$$\frac{\partial \psi}{\partial x}\frac{\partial}{\partial y}(\nabla^2\psi) - \frac{\partial \psi}{\partial y}\frac{\partial}{\partial x}(\nabla^2\psi) + (1+K)\nabla^4\psi + K\nabla^2 N = 0 \tag{12}$$

$$\frac{\partial \dot{\psi}}{\partial y}\frac{\partial N}{\partial x} - \frac{\partial \psi}{\partial x}\frac{\partial N}{\partial y} = (1+K/2)\nabla^2 N - K(2N + \nabla^2\psi) \tag{13}$$

A physical quantity of interest is the skin friction coefficient which is defined as

$$C_f = \frac{\bar{\tau}_w}{\rho a v} \tag{14}$$

where the skin friction $\bar{\tau}_w$ is given by

$$\bar{\tau}_w = \left[(\mu+\kappa)\left(\frac{\partial \bar{u}}{\partial \bar{y}} + \frac{\partial \bar{v}}{\partial \bar{x}}\right) + \kappa \bar{N}\right]_{\bar{y}=0} \tag{15}$$

Using the non-dimensional variables (6) it can be shown that the skin friction coefficient C_f can be written as

$$C_f = \left[(1+K)\left(\frac{\partial^2 \psi}{\partial y^2} - \frac{\partial^2 \psi}{\partial x^2}\right) + KN\right]_{y=0} \tag{16}$$

3. Orthogonal flow

In this case the boundary conditions of Eqs. (12) and (13) are

$$\begin{aligned} &\psi = \frac{\partial \psi}{\partial y} = 0, \quad N = -n\nabla^2\psi \quad \text{on } y = 0 \\ &\psi \sim xy, \quad N \to 0 \quad \text{as } y \to \infty \end{aligned} \tag{17}$$

where n is a constant such that $0 \leqslant n \leqslant 1$. It should be mentioned that the case $n = 0$, called strong concentration by Guram and Smith [19], indicating $N = 0$ near the wall, represents concentrated particle flows in which the microelements close to the wall surface are unable to rotate [20]. The case $n = 1/2$ indicates the vanishing of anti-symmetrical part of the stress tensor and denotes weak concentration [21]. The case $n = 1$, as suggested by Peddieson [22], is used for the modeling of turbulent boundary layer flows.

Following the classical solution of Hiemenz [9], we assume that

$$\psi(x,y) = xf(y), \quad N(x,y) = xg(y) \tag{18}$$

Substituting (18) into Eqs. (12) and (13), we obtain, after one integration of Eq. (12), the following ordinary differential equations:

$$(1+K)f''' + ff'' + 1 - f'^2 + Kg' = 0 \tag{19}$$

$$(1+K/2)g'' + fg' - f'g - K(2g + f'') = 0 \tag{20}$$

subject to the boundary conditions (17) which become

$$\begin{aligned} &f(0) = f'(0) = 0, \quad g(0) = -nf''(0) \\ &f'(\infty) = 1, \quad g(\infty) = 0 \end{aligned} \tag{21}$$

where primes denote differentiation with respect to y.

It is worth mentioning that we can take $g = -(1/2)f''$ for $n = 1/2$. Thus, Eqs. (19) and (20) can be reduced to the following equation:

$$(1+K/2)f''' + ff'' + 1 - f'^2 = 0 \tag{22}$$

Table 1
Values of A for an orthogonal stagnation point with different values of K when $n = 0$ and 1/2

K	A	
	$n = 0$	$n = 1/2$
0	−0.647912	−0.647912
	−0.6479004[a]	
	−0.647900[b]	
0.5	−0.786249	−0.724384
1.0	−0.893920	−0.793521
1.5	−0.984152	−0.857100
2.0	−1.063087	−0.916277
2.5	−1.134038	−0.971858
3.0	−1.198994	−1.024427

[a] Results from Tamada [11].
[b] Results from Labropulu et al. [13].

Further, if we introduce the new similarity variables,

$$f(y) = (1 + K/2)^{1/2}\hat{f}(\eta), \quad \eta = (1 + K/2)^{-1/2}y \tag{23}$$

Eq. (22) reduces to the classical equation [9] which describes the flow of a viscous (Newtonian) and incompressible fluid near an orthogonal stagnation point

$$\hat{f}''' + \hat{f}\hat{f}'' + 1 - \hat{f}'^2 = 0 \tag{24}$$

subject to

$$\hat{f}(0) = \hat{f}'(0) = 0, \quad \hat{f}'(\infty) = 1 \tag{25}$$

where primes now denote differentiation with respect to η.

The skin friction coefficient (16) gives

$$C_f = [(1 + (1 - n)K)]xf''(0) \tag{26}$$

if the boundary condition for $g(0)$ from (21) is used.

We notice that the function $f(y)$ behaves as

$$f(y) \sim y + A \tag{27}$$

when $y \to \infty$, where the values of A for several values of material parameter K are given in Table 1 with $n = 0$ and 1/2. The values reported by Tamada [11] and Labropulu et al. [13] for $K = 0$ (Newtonian fluid) have also been included in this table. It is seen that these values are in very good agreement.

4. Oblique flow

Following Stuart [10], it can be assumed that the stream function ψ far from the wall has the form

$$\psi(x, y) = xy + \alpha y^2 \quad \text{as } y \to \infty \tag{28}$$

where α is a constant and the microrotation $N \to const.$ as $y \to \infty$. Expression (28) suggests that Eqs. (12) and (13) have the solution of the form

$$\psi(x, y) = xF(y) + G(y), \quad N(x, y) = xH(y) + T(y) \tag{29}$$

The boundary conditions that $F(y)$, $G(y)$, $H(y)$ and $T(y)$ satisfy are

$$\begin{aligned} &F(0) = F'(0) = 0, \quad G(0) = G'(0) = 0 \\ &H(0) = -nF''(0), \quad T(0) = -nG''(0) \\ &F(y) \sim y, \quad G(y) \sim \alpha y^2, \quad H(y) \sim 0, \quad T(y) \sim -\alpha \quad \text{as } y \to \infty. \end{aligned} \tag{30}$$

Substituting (29) into Eqs. (12) and (13) it results in, after one integration of equation for $F(y)$, the following equations:

$$(1+K)F''' + FF'' + 1 - F'^2 + KH' = 0 \tag{31}$$

$$(1+K)G''' + FG'' - F'G' + KT' = 2\alpha A \tag{32}$$

$$(1+K/2)H'' + FH' - F'H - K(2H + F'') = 0 \tag{33}$$

$$(1+K/2)T'' + FT' - G'H - K(2T + G'') = 0 \tag{34}$$

subject to

$$\begin{aligned} &F(0) = F'(0) = 0, \quad G(0) = G'(0) = 0 \\ &H(0) = -nF''(0), \quad T(0) = -nG''(0) \\ &F'(\infty) = 1, \quad G''(\infty) = 2\alpha, \quad H(\infty) = 0, \quad T(\infty) = -\alpha \end{aligned} \tag{35}$$

We notice that solutions of Eqs. (31) and (33) subject to (35) are identical with those of Eqs. (19) and (20) subject to (21). However, introducing the new variables

$$G'(y) = 2\alpha h(y), \quad T(y) = 2\alpha t(y) \tag{36}$$

Table 2
Values of $f''(0)$, $h'(0)$ and x_0 for different values of K and n

K	$f''(0)$		$h'(0)$		x_0	
	$n=0$	$n=1/2$	$n=0$	$n=1/2$	$n=0$	$n=1/2$
0	1.232627 1.23259[a] 1.232588[b]	1.232627	1.406592 1.406544[b]	1.406592	−2.282266	−2.282266
0.5	0.992657	1.102486	1.305981	1.406579	−2.631283	−2.551648
1.0	0.841085	1.006423	1.230837	1.406572	−2.926785	−2.795190
1.5	0.736835	0.931764	1.174002	1.406569	−3.186609	−3.019151
2.0	0.660479	0.871584	1.129859	1.406566	−3.421331	−3.227608
2.5	0.601906	0.821736	1.094646	1.406563	−3.637263	−3.423396
3.0	0.555374	0.779566	1.065887	1.406561	−3.838448	−3.608575

[a] Results from Tamada [11].
[b] Results from Labropulu et al. [13].

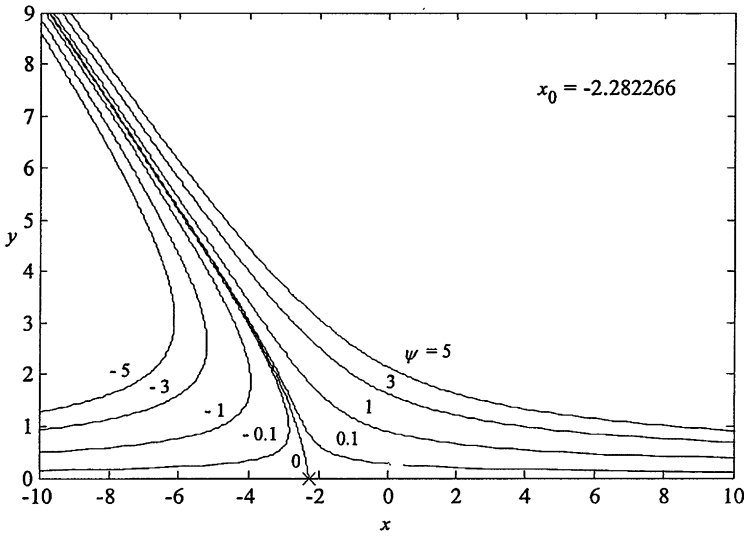

Fig. 1. Streamline pattern for $K=0$ and $n=0$.

Eqs. (32) and (34) can be written as

$$(1+K)h''+Fh'-F'h+Kt'=A \tag{37}$$

$$(1+K/2)t''+Ft'-Hh-K(2t+h')=0 \tag{38}$$

and the boundary conditions (35) give

$$\begin{aligned} &h(0)=0, \quad t(0)=-nh'(0)\\ &h'(\infty)=1, \quad t(\infty)=-1/2 \end{aligned} \tag{39}$$

Employing (29), (36) and (39), the skin friction coefficient given by Eq. (16) can now be written as

$$C_f=[(1+(1-n)K)][xF''(0)+2\alpha h'(0)] \tag{40}$$

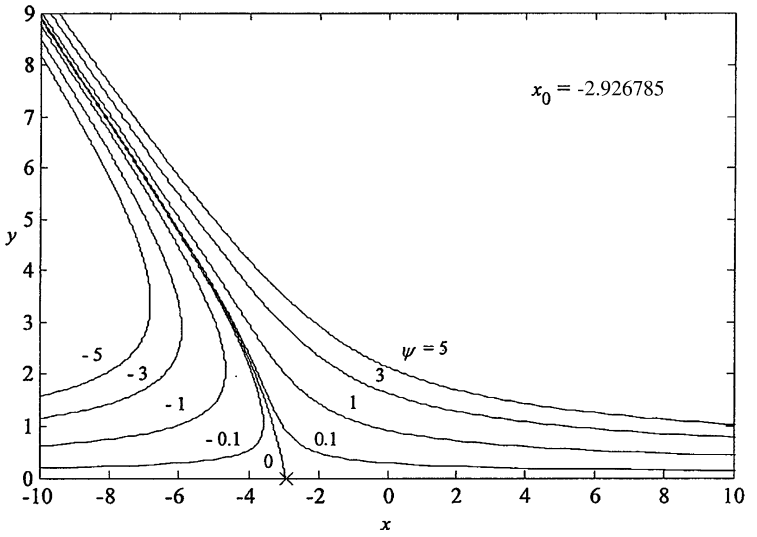

Fig. 2. Streamline pattern for $K=1$ and $n=0$.

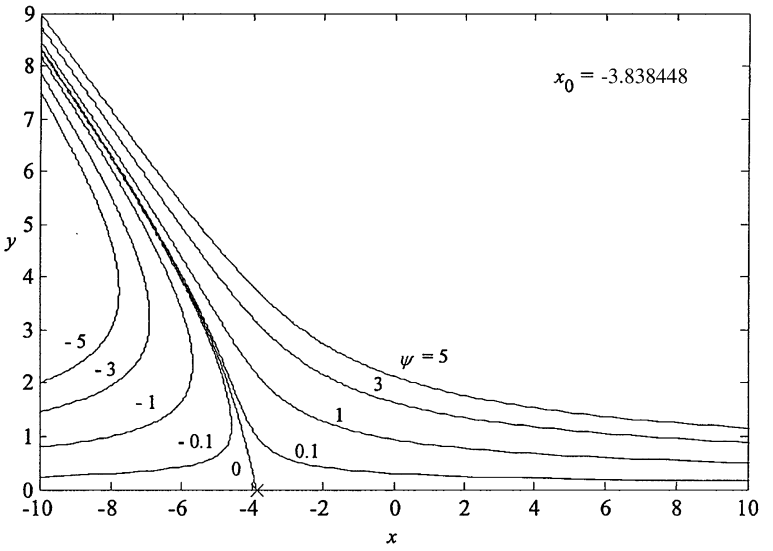

Fig. 3. Streamline pattern for $K=3$ and $n=0$.

where values of $F''(0)$ and $h'(0)$ can be calculated for some values of the parameters K and n. Some streamlines as calculated from (29) taking $\alpha = 1$ can be calculated for different values of K and n. In particular, the streamlines $\psi = 0$ meets the wall at $x = x_0$ (point of stagnation and zero skin friction) where, from (40), x_0 is given by

$$x_0 = -2h'(0)/F''(0) \tag{41}$$

where $F''(0) = f''(0)$ because solutions of Eqs. (31) and (33) subject to (35) are identical with those of Eqs. (19) and (20) subject to (21).

5. Results and discussion

Eqs. (19), (20), (37) and (38) subject to the boundary conditions (21) and (39) have been solved numerically for the material parameter K when the parameter n takes the values $n = 0$ (strong concentration) and $n = 1/2$

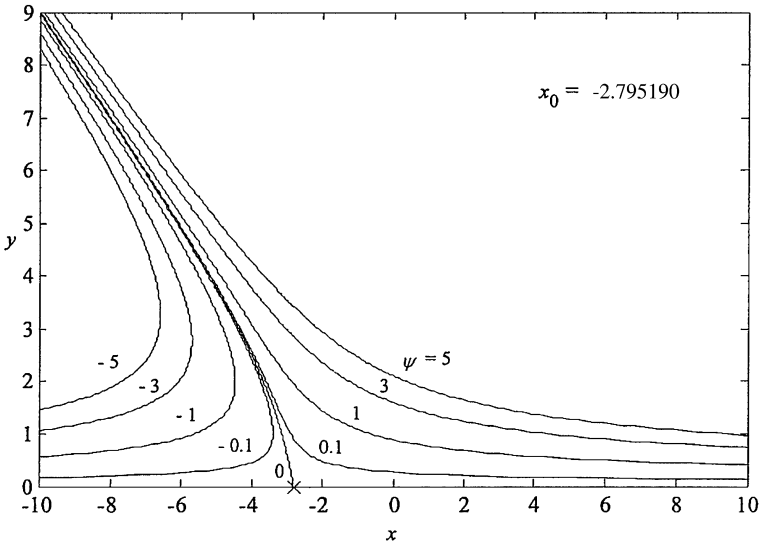

Fig. 4. Streamline pattern for $K = 1$ and $n = 1/2$.

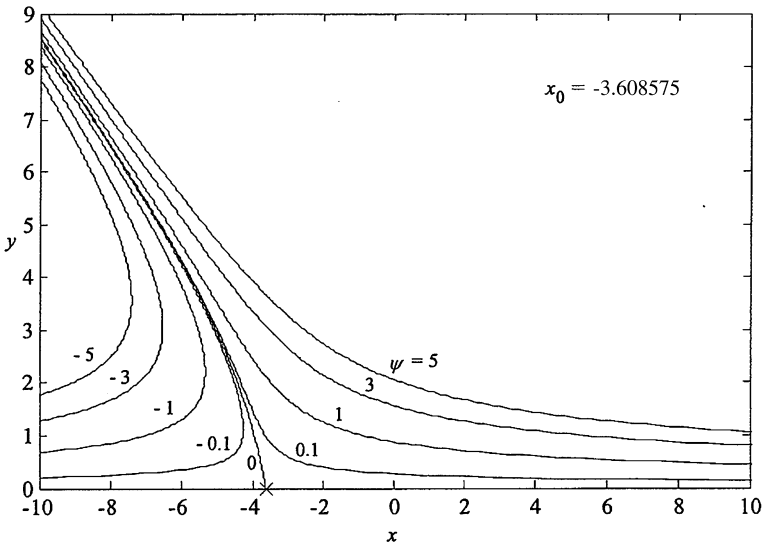

Fig. 5. Streamline pattern for $K = 3$ and $n = 1/2$.

(weak concentration), respectively, using the Keller-box method in conjunction with the Newton's linearization technique as described by Cebeci and Bradshaw [23]. This method has been very successfully used recently by the present authors in solving of some important micropolar problems [24–26]. Values of K considered are $K = 0$ (Newtonian fluid), 0.5, 1.0, 1.5, 2.0, 2.5 and 3.0. For calculation and graphing purposes we took $\alpha = 1$.

Table 2 shows the values of $f''(0)$, $h'(0)$ and x_0 for some values of K and n. Results found by Tamada [11] and Labropulu et al. [13] are also included in this table. We can see that the agreement between the present results of $f''(0)$ and those of Tamada [11] and Labropulu et al. [13] are very good. We will not give values of $g(0)$ and $t(0)$ here because they can be obtained very easily once we get $f''(0)$ and $h'(0)$. They result in from the boundary conditions Eqs. (21) and (39) where we have $g(0) = -nf''(0)$ and $t(0) = -nh'(0)$. It is noticed from Table 2 that the effect of increasing values of material parameter K results in a decrease in values of reduced skin friction $f''(0)$ and also the values are greater for $n = 1/2$ than for $n = 0$. This indicates that the micropolar fluid displays a reduction in drag when compared to the Newtonian fluids (see [27–29]).

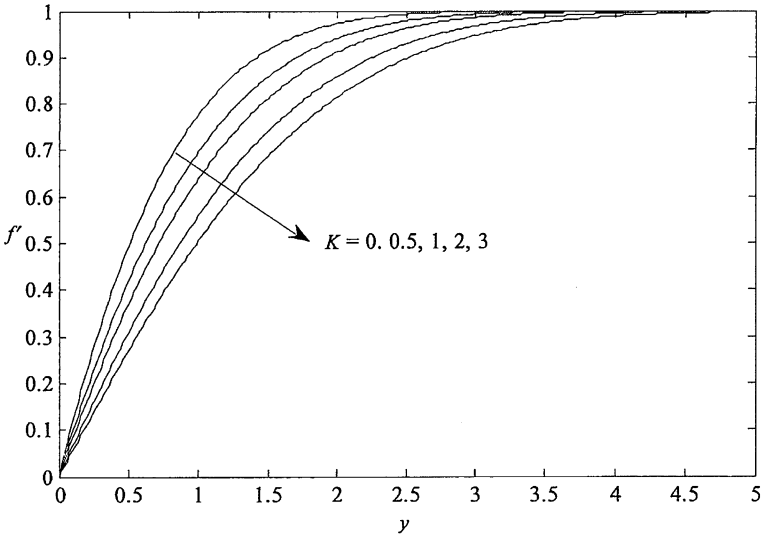

Fig. 6. Velocity profiles f' for different values of K and $n = 0$.

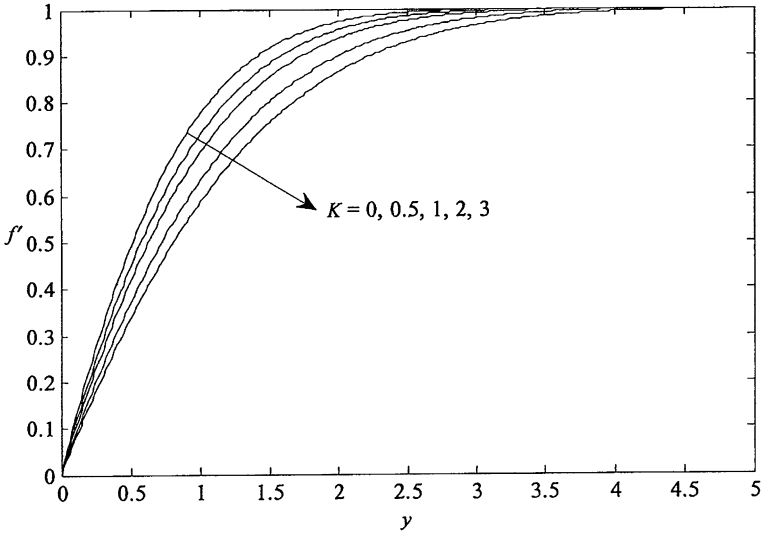

Fig. 7. Velocity profiles f' for different values of K and $n = 1/2$.

The streamline patterns for the oblique flows are shown in Figs. 1–5. The streamline $\psi = 0$ meets the wall $y = 0$ at $x = x_0$, where x_0 is the point of stagnation and zero skin friction. It can be seen from Table 2 and Figs. 1–5 that the stagnation point is at the left of the origin for all the values of $K = 0$ (Newtonian fluid) and $K \neq 0$ (micropolar fluid), and the magnitude of x_0 increases as K increases. The shifting of x_0 depends upon the magnitudes of K and n.

The velocity and microrotation profiles $f'(y)$ and $-g(y)$ are shown in Figs. 6–9 for various values of K when $n = 0$ and 1/2. We notice from Figs. 6 and 7 that as the values of K increase, values of $f'(y)$ near the wall are decreasing. Consequently, the velocity gradient at the wall decreases as K increases. This describes very well the trend of the values of $f''(0)$ obtained in Table 2. On the other hand, profiles for the microrotation $-g(y)$ shown in Fig. 8 suggest that the microrotation increases as K increases for the case when $n = 0$. The peak value of microrotation occurs near the wall then decrease monotonically to zero as y increases. However, for $n = 1/2$ (Fig. 9), the microrotation decreases continuously from its maximum value at the wall to zero far from the

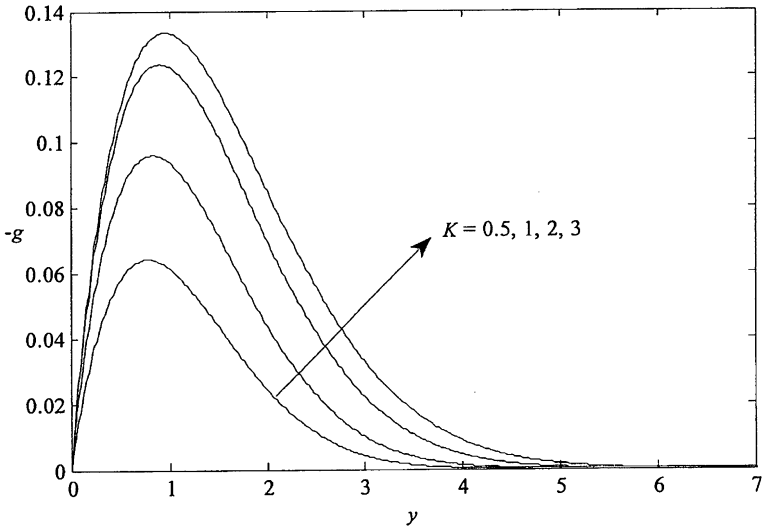

Fig. 8. Microrotation profiles $-g$ for some values of K and $n = 0$.

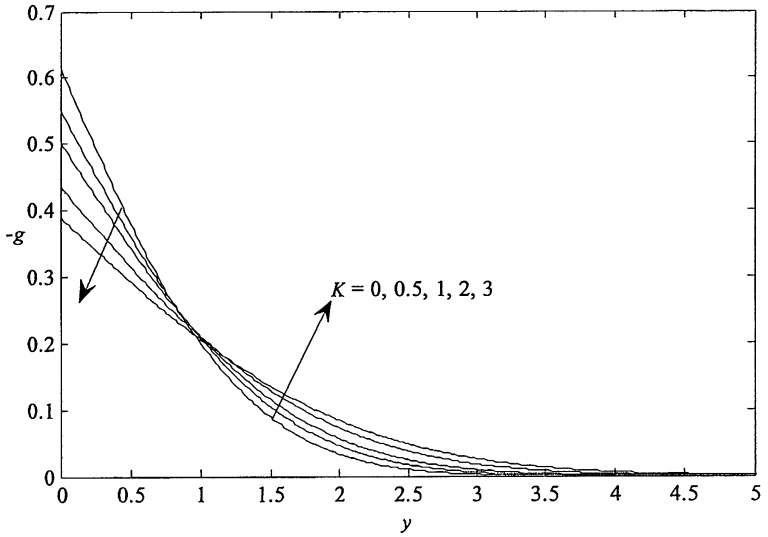

Fig. 9. Microrotation profiles $-g$ for some values of K and $n = 1/2$.

wall. Finally, we notice from Figs. 6 to 9 that, as expected, the velocity and microrotation boundary layer thicknesses increase as the material parameter K increases.

6. Conclusions

A numerical solution of the steady oblique flow of a micropolar fluid impinging on a flat plate is studied. The governing partial differential equations are reduced to a set of ordinary differential equations which are solved numerically for different values of the governing parameters K and n. This solution provides useful information about the steady oblique stagnation-point flow, which agrees qualitatively with that obtained before for the case of a Newtonian fluid. We can see in this paper that the similarity solution for the micropolar fluid has many of the characteristics expected of Newtonian fluid motions. In a subsequent paper, we shall study the steady oblique flow of a micropolar fluid impinging on a flat porous wall with suction or blowing on the wall. The process of suction and blowing has its importance in many engineering activities such as in the design of thrust bearing and radial diffusers, thermal oil recovery, etc. [13].

Acknowledgements

The authors are indebted to the referees for their valuable comments and suggestions which led to the substantial improvement of the paper.

References

[1] A.C. Eringen, Theory of micropolar fluids, J. Math. Mech. 16 (1966) 1–18.
[2] A.C. Eringen, Theory of thermomicrofluids, J. Math. Anal. Appl. 38 (1972) 480–496.
[3] J.W. Hoyt, A.G. Fabula, The effect of additives on fluid friction, U.S. Naval Ordinance Test Station Report, 1964.
[4] T. Ariman, M.A. Turk, N.D. Sylvester, Microcontinuum fluid mechanics – a review, Int. J. Engng. Sci. 11 (1973) 905–930.
[5] T. Ariman, M.A. Turk, N.D. Sylvester, Application of microcontinuum fluid mechanics, Int. J. Engng. Sci. 12 (1974) 273–293.
[6] G. Łukaszewicz, Micropolar Fluids: Theory and Application, Birkhäuser, Basel, 1999.
[7] A.C. Eringen, Microcontinuum Field Theories. II: Fluent Media, Springer, New York, 2001.
[8] C.Y. Wang, The unsteady oblique stagnation point flow, Phys. Fluids 28 (1985) 2046–2049.
[9] K. Hiemenz, Die Grenzschicht an einem in den gleichförmigen Flüssigkeitsstrom eingetauchten geraden Kreiszylinder, Dingier Polytech. J. 326 (1911) 321–324.
[10] J.T. Stuart, The viscous flow near a stagnation point when the external flow has uniform vorticity, J. Aerospace Sci. 26 (1959) 124–125.
[11] K.J. Tamada, Two-dimensional stagnation point flow impinging obliquely on a plane wall, J. Phys. Soc. Jpn. 46 (1979) 310–311.
[12] J.M. Dorrepaal, An exact solution of the Navier–Stokes equation which describes non-orthogonal stagnation-point flow in two dimensions, J. Fluid Mech. 163 (1986) 141–147.
[13] F. Labropulu, J.M. Dorrepaal, O.P. Chandna, Oblique flow impinging on a wall with suction or blowing, Acta Mech. 115 (1996) 15–25.
[14] N. Takemitsu, Y. Matunobu, Unsteady stagnation-point flow impinging obliquely on an oscillating flat plate, J. Phys. Soc. Jpn. 47 (1979) 1347–1353.
[15] J.M. Dorrepaal, O.P. Chandna, F. Labropulu, The flow of visco-elastic fluid near a point of reattachment, J. Appl. Math. Phys. (ZAMP) 43 (1992) 708–714.
[16] B.S. Tilley, P.D. Weidman, Oblique two-fluid stagnation-point flow, Eur. J. Mech. B/Fluids 17 (1998) 205–217.
[17] D.A.S. Rees, A.P. Bassom, The Blasius boundary-layer flow of a micropolar fluid, Int. J. Engng. Sci. 34 (1996) 113–124.
[18] D.A.S. Rees, I. Pop, Free convection boundary-layer flow of a micropolar fluid from a vertical flat plate, IMA J. Appl. Math. 61 (1998) 179–197.
[19] G.S. Guram, C. Smith, Stagnation flows of micropolar fluids with strong and weak interactions, Comp. Math. Appl. 6 (1980) 213–233.
[20] S.K. Jena, M.N. Mathur, Similarity solutions for laminar free convection flow of a thermomicropolar fluid past a nonisothermal flat plate, Int. J. Engng. Sci. 19 (1981) 1431–1439.
[21] G. Ahmadi, Self-similar solution of incompressible micropolar boundary layer flow over a semi-infinite plate, Int. J. Engng. Sci. 14 (1976) 639–646.
[22] J. Peddieson, An application of the micropolar fluid model to the calculation of turbulent shear flow, Int. J. Engng. Sci. 10 (1972) 23–32.
[23] T. Cebeci, P. Bradshaw, Physical and Computational Aspect of Convective Heat Transfer, Springer, New York, 1984.
[24] Y.Y. Lok, P. Phang, N. Amin, I. Pop, Unsteady boundary layer flow of a micropolar fluid near the forward stagnation point of a plane surface, Int. J. Engng. Sci. 41 (2003) 173–186.

[25] Y.Y. Lok, N. Amin, I. Pop, Unsteady boundary layer flow of a micropolar fluid near the rear stagnation point of a plane surface, Int. J. Thermal Sci. 42 (2003) 995–1001.
[26] Y.Y. Lok, N. Amin, I. Pop, Steady two-dimensional asymmetric stagnation point flow of a micropolar fluid, Z. Angew. Math. Mech. (ZAMM) 83 (2003) 594–602.
[27] R.S.R. Gorla, Boundary layer flow of a micropolar fluid in the vicinity of an axisymmetric stagnation point on a cylinder, Int. J. Engng. Sci. 28 (1990) 145–152.
[28] I.A. Hassanien, R.S.R. Gorla, Combined forced and free convection in stagnation flows of micropolar fluids over vertical non-isothermal surfaces, Int. J. Engng. Sci. 28 (1990) 783–792.
[29] R. Bhargava, L. Kumar, H.S. Takhar, Finite element solution of mixed convection micropolar flow driven by a porous stretching sheet, Int. J. Engng. Sci 41 (2003) 2161–2178.